Geophysical Research Letters

RESEARCH LETTER
10.1029/2018GL078079

Key Points:
- This study compares the real-time performance of two earthquake early warning systems (EEWS) for the 2018 Hualian earthquake
- The classification performance rates of the on-site EEWS are 60% and 40% should a reasonable tolerance range be accepted
- No correct alerts were issued in time by the regional EEWS, even after a reasonable tolerance range was accepted

Supporting Information:
- Supporting Information S1
- Figure S1
- Figure S2
- Figure S3
- Figure S4
- Figure S5
- Figure S6
- Figure S7
- Figure S8

Correspondence to:
T. Y. Hsu,
tyhsu@mail.ntust.edu.tw

Citation:
Hsu, T. Y., Lin, P. Y., Wang, H. H., Chiang, H. W., Chang, Y. W., Kuo, C. H., et al. (2018). Comparing the performance of the NEEWS earthquake early warning system against the CWB system during the 6 February 2018 M_w 6.2 Hualien earthquake. *Geophysical Research Letters*, *45*. https://doi.org/10.1029/2018GL078079

Received 27 MAR 2018
Accepted 11 JUN 2018
Accepted article online 21 JUN 2018

Comparing the Performance of the NEEWS Earthquake Early Warning System Against the CWB System During the 6 February 2018 M_w 6.2 Hualien Earthquake

T. Y. Hsu[1,2], P. Y. Lin[2], H. H. Wang[2], H. W. Chiang[2], Y. W. Chang[2], C. H. Kuo[2], C. M. Lin[2], and K. L. Wen[2,3]

[1]Department of Civil and Construction Engineering, National Taiwan University of Science and Technology, Taipei, Taiwan, [2]National Center for Research on Earthquake Engineering, Taipei, Taiwan, [3]Department of Earth Sciences, National Central University, Taoyuan, Taiwan

Abstract The National Center for Research on Earthquake Engineering, Taiwan, has developed an Earthquake Early Warning System (NEEWS). The NEEWS predicts peak ground acceleration (PGA) using an on-site approach, whereas the Central Weather Bureau (CWB), Taiwan, uses a regional approach. Earthquake alerts are issued at the NEEWS stations once PGA reaches a preassigned PGA threshold, regardless of the approach used. An earthquake with a magnitude of 6.2 and a focal depth of 10.0 km struck Hualien, in eastern Taiwan, on 6 February 2018. It resulted in 17 fatalities and 285 injuries, 4 collapsed buildings, and damage to more than 175 buildings. During the earthquake, the system performance of 28 NEEWS stations was documented. In this study, we compare and discuss the accuracy of the PGA predictions, lead times, and classification performance of both approaches.

Plain Language Summary The National Center for Research on Earthquake Engineering, Taiwan, has developed an Earthquake Early Warning System (NEEWS). The NEEWS predicts peak ground acceleration (PGA) using an on-site approach, whereas the Central Weather Bureau (CWB), Taiwan, uses a regional approach. Earthquake alerts are issued at the NEEWS stations once PGA reaches a preassigned PGA threshold, regardless of the approach used. On 6 February 2018, an earthquake with a magnitude of 6.2 and a focal depth of 10.0 km struck Hualien, in eastern Taiwan. It resulted in 17 fatalities and 285 injuries, 4 collapsed buildings, and damage to more than 175 buildings. During the earthquake, the system performance of 28 NEEWS stations was documented. In this study, we compare and discuss the accuracy of the PGA predictions, lead times, and classification performance of both approaches.

1. Introduction

Taiwan is highly susceptible to seismic hazards from inland earthquakes. In addition to the 33 known active faults in Taiwan (as published by the Central Geological Survey), unknown inland faults may also trigger severe casualties and property loss (e.g., the Meinong earthquake in southern Taiwan resulted in 117 casualties and 247 damaged buildings in 2016). Consequently, earthquake alerts provided by a regional early earthquake warning (EEW) system may not always be issued on time, especially near epicentral sites, where the ground motion is typically strongest and begins shortly after the earthquake onset.

The National Center for Research on Earthquake Engineering (NCREE), Taiwan, has been developing an on-site EEW system since 2009 to provide increased lead times for regions with a higher likelihood of sustaining damage (i.e., regions near epicenter). The on-site EEW approach has recently been the subject of numerous studies worldwide (Allen et al., 2009; Böse et al., 2012; Carranza et al., 2013; Caruso et al., 2017; Emolo et al., 2016; Hsu et al., 2013; Kanamori, 2005; Nakamura, 1998; Odaka et al., 2003; Peng et al., 2015; Wu et al., 2013; Zollo et al., 2010). The NCREE implemented an on-site Early Earthquake Warning System (NEEWS) by first establishing several stations in elementary schools with a limited budget. The system performed relatively well during a number of moderate earthquakes in 2013. Therefore, in late 2014, the Ministry of Education as well as the Ministry of Science and Technology in Taiwan began rolling out the NEEWS to all public elementary and junior high schools in Taiwan. Approximately 90 NEEWS stations are planned for implementation in order to provide earthquake alerts to 3,400 schools by the end of 2018.

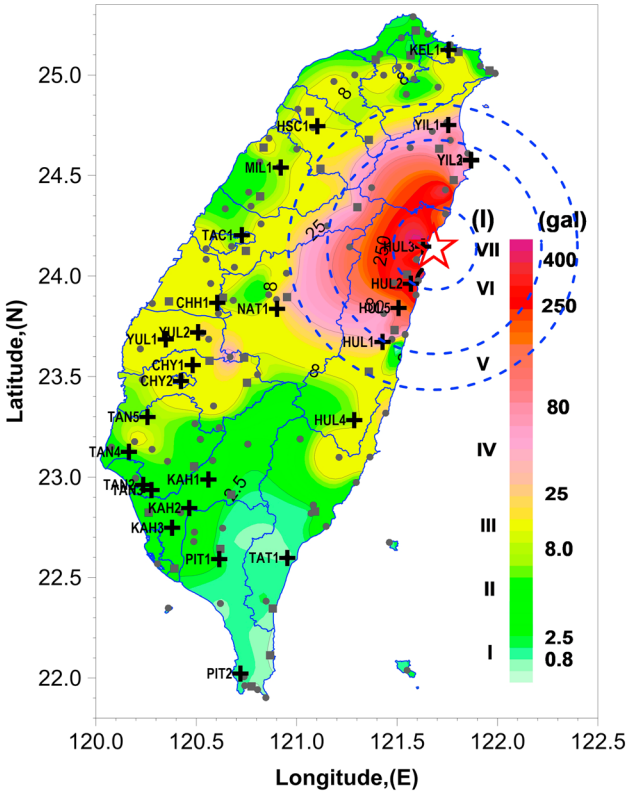

Figure 1. Location of the 28 NEEWS stations (black cross), 101 RTD stations (gray circle), and 32 SANTA stations (gray square). The background is the distribution of the observed PGA values at all CWB RTD, SANTA, and NEEWS stations. The star indicates the epicenter location. The inner circle with a radius of 23 km, the middle circle with a radius of 55 km, and the outer circle with a radius of 75 km roughly delineate the blind zone of the NEEWS system, that of the CWB EEW system, and the observed region where the NEEWS-issued alert was faster than the CWB EEW counterpart, respectively. The scale bar shows the correspondence of the CWB intensity scale (Wu et al., 2003) employed in Taiwan, with horizontal PGA values. NEEWS = NCREE Early Earthquake Warning System; NCREE = National Center for Research on Earthquake Engineering; RTD = Real-Time Digital; SANTA = Seismic Array of NCREE in Taiwan; PGA = peak ground acceleration; CWB = Central Weather Bureau; EEW = early earthquake warning.

The NEEWS estimates the peak ground acceleration (PGA) of an imminent earthquake from the same station by relying on a recently developed support vector machine (SVM) technique. To predict the PGA using a SVM prediction model, once triggered, six *P* wave features of the vertical component of a single NEEWS seismic station with a 3-s window are used. These features include the predominant period, peak acceleration amplitude, peak velocity amplitude, peak displacement amplitude, cumulative absolute velocity, and the integral of the squared velocity. We used some representative earthquake records from the Taiwan Strong Motion Instrumentation Program (for the 1992–2006 period) to train and validate the SVM prediction model. Afterward, we tested the constructed model using all the earthquake records from the same period; the results were quite promising. During the Meinong earthquake in 2016, which had a moment magnitude of 6.5, the performance of the NEEWS was remarkable, the details of which have been summarized and published (Hsu et al., 2013, 2016). In 2017, SIGMU Disaster Prevention Technology (SIGMU DPT), a private company, began collaborating with the NCREE and established a network system that receives alert information from both the NEEWS and the regional EEW, run by the Central Weather Bureau (CWB), Taiwan. The CWB regional EEW system needs at least six picks of seismic waveforms from the CWB Real-Time Digital (RTD) seismic stations to locate an event. In general, at least 12 s is required after an earthquake to estimate the hypocenter.

The Hualien earthquake (M_w = 6.2) occurred at 11:50 p.m. local time, on 6 February 2018 (3:50 p.m. UTC), at 24.14°N latitude, 121.69°E longitude, with a focal depth of 10.0 km. The earthquake resulted in 17 deaths, 285 injuries, 4 collapsed buildings, and damage to more than 175 buildings. It provided an opportunity for a practical comparison of the in situ performance between the on-site EEW (by the NEEWS) and its regional counterparts (by the CWB). Therefore, the purposes of this study were to elucidate how the NEEWS functions and to compare the performance of the two EEW systems, with the Hualien earthquake as the case study.

2. Data on the Hualien Earthquake

During the Hualien earthquake, 101, 32, and 28 valid acceleration time histories were recorded at the CWB RTD stations, the Seismic Array of NCREE in Taiwan (SANTA) stations, and the NCREE NEEWS, respectively. The largest measured horizontal PGA value was 482.36 Gal, which was observed at the CWB ETL station, located approximately 7 km west of the epicenter. Based on the focal mechanism solutions calculated by the CWB and the U.S. Geological Survey, the source rupture plane of the main shock was likely a north-south striking (209°) fault dipping 73° toward the south, with a left-lateral strike slip; the offset was predominantly horizontal and parallel to the fault trace.

The distribution of the observed PGA values at all the CWB RTD stations, the SANTA stations, and the NEEWS stations is shown in Figure 1. The locations of these stations are also plotted in the same figure. The region with PGAs higher than 250 Gal evidently extends from the epicenter to the southwest, along the direction of the Milun fault, as marked with the thick black solid line near Station HUL2. The strong ground motion distribution may have resulted from the southwestward rupture of the left-lateral strike-slip fault. Data on all the stations are listed in summary form under Table 1.

During the Hualian earthquake, because the epicenter was outside the region covered by the CWB RTD seismic network, waveforms from more stations were required to locate the hypocenter. The alert was issued based on seismic waveforms from 12 CWB RTD stations. Moreover, the density of the CWB RTD stations in the Hualian region is relatively small, as shown in Figure 1. Consequently, after the Hualian earthquake struck, the CWB EEW system took 17 s to issue an alert.

Table 1
Performance Summary of the NEEWS and CWB EEW System at 28 NEEWS Stations During the Hualien Earthquake

					NEEWS			CWB		
Station name	Epicenter distance(km)	Measured PGA (Gal)	Measured intensity	Alarm threshold	Lead time (s)	Predicted PGA (Gal)	Predicted intensity	Lead time (s)	Predicted PGA (Gal)	Predicted intensity
HUL3	6.2	244.9	5	5	−2.8	286.6	6	−16.7	785.4	7
HUL2	23.2	219.0	5	5	−0.1	219.7	5	−11.1	219.2	5
HUL5	37.9	118.5	5	5	3.2	37.2	4	−4.7	119.7	5
YIL2	51.6	81.7	5	5	4.4	39.4	4	−1.5	84.3	5
YIL3	51.8	112.3	5	5	3.6	25.9	4	−2.4	83.7	5
HUL1	58.1	32.2	4	5	4.4	41.7	4	0.4	58.6	4
YIL1	68.2	30.5	4	5	7.2	57.3	4	5.3	55.4	4
NAT1	86.9	12.9	3	4	7.1	2.0	1	8.1	22.8	3
MIL1	89.7	7.1	2	4	4.6	13.3	3	7.7	24.0	3
HSC1	89.8	7.7	2	4	5.4	20.5	3	8.5	39.1	4
TAC1	98.1	6.9	2	4	12.8	9.3	3	16.9	24.4	3
HUL4	103.3	6.3	2	5	14.5	1.9	1	18.6	16.4	3
KEL1	109.4	7.1	2	4	8.8	7.6	2	13.9	21.8	3
CHH1	114.4	8.7	3	4	13.8	6.0	2	19.9	20.6	3
YUL2	128.8	13.6	3	4	12.1	8.5	3	24.2	23.4	3
CHY1	138.9	11.0	3	4	15.5	3.0	2	26.6	21.4	3
YUL1	145.5	10.5	3	4	15.9	0.9	1	27.9	19.1	3
CHY2	148.3	12.0	3	4	13.5	1.0	1	28.5	20.4	3
KAH1	171.9	3.8	2	4	16.4	4.6	2	36.5	7.6	2
TAN5	173.2	6.5	2	4	17.5	0.5	0	29.4	13.9	3
TAT1	186.5	1.0	1	4	15.9	0.4	0	36.0	8.9	3
KAH2	190.1	4.3	2	4	14.8	19.1	3	44.2	5.5	2
TAN4	191.9	5.0	2	4	14.7	0.5	0	26.7	14.0	3
TAN3	196.4	4.5	2	4	0.0	0.0	—	50.1	10.8	3
TAN2	197.6	4.9	2	4	7.8	0.3	0	29.9	10.5	3
PIT1	203.7	2.6	2	5	0.0	0.0	—	51.1	7.1	2
KAH3	204.1	3.0	2	4	20.9	0.5	0	47.9	6.6	2
PIT2	254.6	2.1	1	5	−11.2	10.3	3	60.4	5.7	2

Note. NEEWS = NCREE Early Earthquake Warning System; NCREE = National Center for Research on Earthquake Engineering; CWB EEW = Central Weather Bureau early earthquake warning; PGA = peak ground acceleration.

3. Performance and Discussion

Basic information as well as the performance metrics for the NEEWS and the CWB EEW systems are listed under Table 1. First, we considered the accuracy of the predicted PGA during the Hualien earthquake. Figure 2 displays a comparison of the predicted and measured PGA values of all 28 stations. The figure shows that overall, the predicted PGA values for both the NEEWS and CWB correspond to the measured PGA value relatively well, at least on a logarithmic scale. The standard deviation of the difference between the predicted PGA of the NEEWS and the measured PGA was approximately 26.2 Gal, whereas that between the predicted PGA of the CWB and the measured PGA was approximately 101.1 Gal. The large standard deviation of the CWB results is due to an overestimated PGA value of 785.4 Gal at Station HUL3 with epicenter distance only 6.2 km, despite the measured PGA being only 244.9 Gal. The standard deviation of the NEEWS and CWB decreased to 24.9 and 10.8 Gal, respectively, when Station HUL3 was excluded.

An eight-level intensity scale is used to assess CWB seismic intensity based on the measured PGA (Wu et al., 2003). Regarding the difference in CWB seismic intensity, when used as the basis for issuing an alert for general applications, the same figure shows that the intensity difference for most stations is within the range of a ±1 intensity level, except for those of the NEEWS, with a measured intensity of less than 4. The rate of the accurately predicted intensity values for the NEEWS alerts was 18/28 = 64.3%, whereas that of the CWB alerts was 25/28 = 89.3%. However, if the measured seismic intensity was smaller than the preassigned threshold, in practice this underestimated intensity case did not have an effect. If only the measured and predicted seismic intensities with an intensity 4 and above were considered, the rate of accurate predicted intensity of the NEEWS became 7/7 = 100%, whereas that of the CWB became 6/8 = 75%. The denominator of the CWB

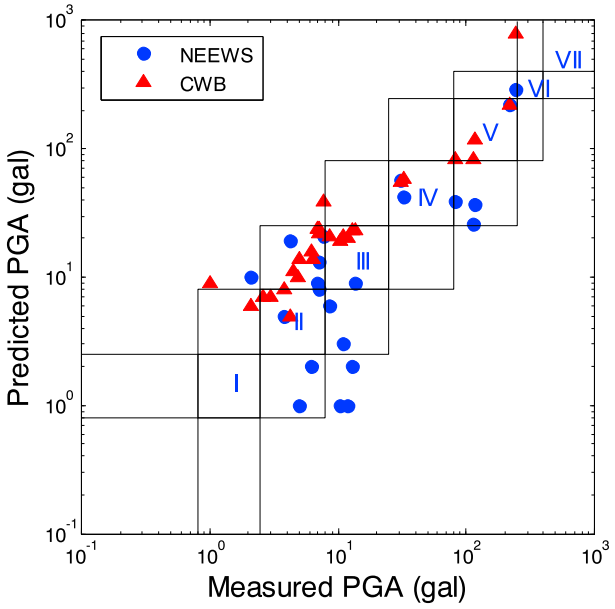

Figure 2. Distribution of measured and predicted PGA values for the 28 NEEWS stations. The predicted PGA values correspond to the measured PGA values relatively well on a logarithmic scale. The standard deviation of the difference between predicted and measured PGA values is approximately 26.2 Gal and for the NEEWS and CWB EEW system is 101.1 Gal (see text for more details). PGA = peak ground acceleration; NEEWS = NCREE Early Earthquake Warning System; NCREE = National Center for Research on Earthquake Engineering; CWB EEW = Central Weather Bureau early earthquake warning.

became 8, because the predicted intensity was 4 at Station HSC1. The incorrect prediction in the CWB at Station HUL3, with a predicted intensity of 7 and a measured intensity of 5, is actually acceptable in practice, because the predicted intensity is larger than the threshold, and an alert can still be issued.

The measured acceleration time history of the horizontal component with the maximum PGA at all stations is shown in supporting information Figures S1 to S7, sequenced by the epicenter distance. The *S* wave arrival, time at trigger, and alert issuance of the NEEWS are also marked in the same figure. The lead time is defined as the interval from when a PGA prediction is first issued until the arrival of the *S* wave. At Station HUL3, with only a 6.2-km epicenter distance, the lead time of the NEEWS was −2.8 s (Figure S1). At Station HUL2, which is near the region that sustained serious damage (with an approximate 23.2 km epicenter distance), the lead time of the NEEWS was close to 0 (i.e., −0.1 s). The current version of the NEEWS, using 3 s after the *P* wave arrival, seemed to have a blind zone with a radius of approximately 23 km during the Hualian earthquake.

The other stations, those with a seismic intensity of 5 (i.e., HUL5, YIL2, and YIL3), recorded approximately 3 to 4 s of lead time, with an epicenter distance that measured approximately 40 to 50 km. The relationship between the lead time and the epicenter distance of the NEEWS and the CWB is displayed in Figure 3 and Table 1. They show that the lead time generally increases with the epicenter distance. (The trends of most of the stations using both approaches are represented with a dashed and a dash-dotted line, respectively, in the figure.) In addition, Figure 3 shows that four NEEWS stations (solid triangles) exhibit trends that are relatively different from those reported by the other stations. This is probably due to a poor signal-to-noise ratio as well as a PGA value lower than 5 Gal at these stations. The *P* wave seems to have been too small to trigger the system, which was ultimately triggered by the arrival of waves with a larger amplitude. Fortunately, the PGA value of these stations does not reach the threshold for triggering an alert. Since an alert does not have to be issued at these stations, this approach does not have any negative practical consequences.

Moreover, we observed that within approximately 75 km of the epicenter distance, the lead time of the NEEWS alerts were larger than those of the CWB system. The area within the range with the 75-km radius and epicenter as the center is plotted in Figure 1. Evidently, the NEEWS system can gain more lead time for the area with a higher seismic intensity. In contrast, the CWB alerts gain more lead time for the area with a larger epicenter distance. We believe that the EEW alerts can be deemed societally *successful* if users can gain 3–4 s to (i) notice the alert, (ii) decide which actions to take, and (iii) take action. Of course, electronic systems would not be subject to such limitations.

As Hsu et al. (2016) noted in detailing the performance of the NEEWS during the 5 February 2016 M_w 6.53 Meinong earthquake, the preassigned intensity threshold of the stations (i.e., $\bar{I}_i$, in eastern Taiwan, specifically Yilan County, Hualien County, and Taitung County), was set as intensity 5, whereas for the other stations it was set to 4.

To evaluate the predictive ability of a site about to experience an above- and below-threshold PGA, we modified the definition of *classification performance* provided by Meier (2017). If an alert was issued before the threshold was reached, we considered it a true positive (*TP*), and the resulting warning time was valid. Conversely, if an alert was issued but the ground motion never reached the threshold, we considered it a false positive (*FP*). If the final ground motion amplitude reached the threshold but no alert was issued on time, then we considered it a false negative (*FN*). Even when the alert was issued after the threshold was reached, it was still considered an FN. Because the fraction of true negative cases is relatively arbitrary (Meier, 2017; i.e., too easy to achieve the correct results), we focused only on the TP, FP, and FN cases in this study.

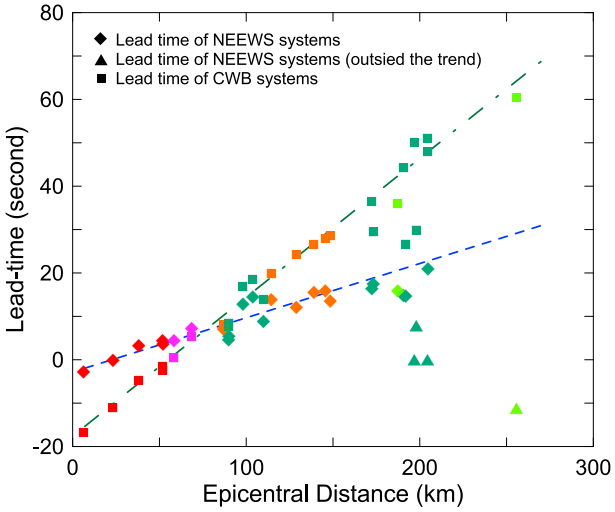

Figure 3. Correlation between lead time and epicenter distance at the 28 NEEWS stations. The solid diamonds and triangles represent the NEEWS lead time, and the dashed blue line indicates the general trend for most of the stations. The solid squares represent the lead time of the CWB EEW system, and the green dashes delineate the general trend for most of the stations. The red, pink, orange, green, and light green solid shapes represent the measured CWB intensities of 5, 4, 3, 2, and 1, respectively. The NEEWS lead time of the four stations in solid triangles fall outside the trend, probably due to a poor signal-to-noise ratio, with a PGA value lower than 5 Gal. NEEWS = NCREE Early Earthquake Warning System; NCREE = National Center for Research on Earthquake Engineering; CWB EEW = Central Weather Bureau early earthquake warning; PGA = peak ground acceleration.

During the Hualien earthquake, according to the preassigned threshold at each station, the classification performance of the TP, FN, and FP rates for the NEEWS was 0%, 100%, and 0%, respectively. The 0% TP rate is due to the overly short epicenter distance for Stations HUL3 and HUL2 (i.e., less than 25 km), and thus, they had no lead time, even though they had highly accurate predicted PGA values. Moreover, although approximately 3 to 4 s of lead time was achieved for Stations HUL5, YIL2, and YIL3, no alert was issued because of an underestimated predicted PGA. However, the TP, FN, and FP rates of the CWB were 0%, 83.3%, and 16.7%, respectively. Although the predicted PGAs reached the threshold for the stations (i.e., HUL3, HUL2, HUL5, YIL2, and YIL3), no positive lead time was secured by the CWB EEW system, because the alert was issued after the arrival of the *S* wave. For Station HSC1, the measured intensity was only 2, but the predicted intensity was 4; hence, an FP alert was issued by the CWB EEW system.

If a predicted intensity was within a tolerance range of ±1 level, then we treated it as an acceptable misclassification. In other words, if an alert was issued for a site that had an intensity above $\bar{I}_i - 1$, we considered it a TP; only if the measured ground motion was higher than one level below the threshold did we consider it an FP. Likewise, if no alert was issued, we considered it an FN only if the measured intensity exceeded $\bar{I}_i + 1$. The definition of the tolerance range is, of course, debatable and it is subject to different end users' perspectives and allowance. Therefore, the TP, FN, and FP rates of the NEEWS became 60%, 40%, and 0%, respectively, after allowing for this tolerance range. However, the classification performance of the CWB EEW system did not improve, even after we introduced the tolerance range. When the tolerance range was lowered to a mere ±0.5 level, in a manner similar to Meier's suggestion (Caruso et al., 2017), the same improvement in classification performance was obtained for both the NEEWS and CWB EEW systems.

Because the effect of the source direction was not considered in the current embedded PGA prediction algorithm of the NEEWS, the distribution of the PGA difference—defined as the predicted PGA minus the measured PGA—may display the directivity associated with the earthquake source rupture direction (Hsu et al., 2016). Supporting information Figure S8 shows that most of the PGA differences for the region in the south of the epicenter (separated by the dotted red line in supporting information Figure S8) were negative. By contrast, most of the PGA differences for the region in the northern portion were positive. This phenomenon implies the potential existence of directivity for the Hualian earthquake source rupture. In other words, most of the measured PGA values at the stations located south of the epicenter were larger than the predicted PGA value, potentially due to the fault rupture southward from the epicenter. The opposite is true for stations situated in the northern direction. The PGA at Station YIL3 was significantly underpredicted. This station was established in June 2017; hence, only a few earthquakes were recorded. Further study with sufficient earthquake data is required to understand the reason for this PGA underprediction.

4. Conclusion and Future Work

The Hualien earthquake, which resulted in 17 fatalities and damaged more than 175 buildings, provided an occasion to validate the performance of the NEEWS systems. This time, the network system provided by the SIGMU DPT, which issues alerts based on data from both the NEEWS and CWB EEW systems, made it possible to compare the practical in situ performance of the NEEWS against that of the CWB EEW system for the first time in the research literature.

The PGA prediction accuracy for both EEW systems is relatively high. If only the measured and predicted seismic intensities with 4 and above are considered, the rates of accurate predicted intensity for both EEW systems are also relatively high.

The NEEWS currently issues an alert 3 s after it is triggered. The observed radius of the blind zone of the NEEWS during the Hualian earthquake spanned a radius of approximately 23 km, whereas that of the CWB EEW system spanned a radius of approximately 55 km. For a number of NEEWS stations within a region near the epicenter with a measured intensity ≥5, approximately 3 to 4 s of lead time was provided by the NEEWS. The alert issued by the CWB EEW system caught up to the NEEWS alert when the epicenter distance reached approximately 75 km. Nearly the entire region, with a measured PGA exceeding 25 Gal (the CWB intensity was 4 and greater), was located inside the circle. However, the CWB provided a longer and steadier lead time outside the circle.

Although the general performance of the PGA prediction accuracy and intensity prediction for both EEW systems was relatively effective, the ability to issue alerts to sites that are about to experience an above-threshold intensity during the Hualien earthquake was mainly controlled by the lead time provided by these two EEW systems. Based on the metrics suggested by Meier (2017), but adjusted to the conditions native to Taiwan, for the classification performance of the CWB EEW system, the TP, FN, and FP rates were 0%, 83.3%, and 16.7%, respectively.

In other words, no correct alerts were issued on time, but only one FP alert was issued by the CWB, even if a reasonable tolerance range was accepted. By contrast, the classification performance of the NEEWS stations had TP, FN, and FP rates of 60%, 40%, and 0%, respectively, if a reasonable tolerance range is accepted. The NEEWS (developed by the NCREE) apparently has considerable potential for classification performance improvements, especially for regions near an epicenter where damage is more likely to occur. To extend the lead time of the NEEWS, a PGA prediction model using only 1 s of the *P* wave after it is triggered is being validated at a test station, with plans for deployment with the NEEWS stations in the near future. However, during the Hualian earthquake, the populations in areas most affected by this deadly earthquake were concentrated in the blind zone for both systems, even when shorter-window *P* wave detection was used. This is a public reminder that EEW systems have practical limitations, and ensuring a structural seismic capacity to withstand anticipated earthquake is absolutely the foundation for mitigating earthquake loss.

The SIGMU DPT currently issues alerts based on data from both the NEEWS and CWB. During the Hualien earthquake, for the classification performance of the integrated EEW system, the TP, FN, and FP rates were 3/6 = 50.0%, 2/6 = 33.3%, and 1/6 = 16.7%, respectively, if a reasonable tolerance range was accepted. The SIGMU DPT is also installing economical P-Alert EEW devices that were developed by Wu et al. (2013) at National Taiwan University on the same sites of the NEEWS installations. We hope that schools in Taiwan will benefit from an integrated EEW system comprising the NEEWS, CWB, and P-Alert in the near future.

Acknowledgments
This research was supported in part by the Ministry of Science and Technology, Republic of China, under grants MOST 107–2119-M-492-006 and MOST 106–2625-M-011-001. The authors thank the Central Weather Bureau for providing data from the real-time data stations. The authors also thank SIGMU Disaster Prevention Technology for providing EEW information from the NEEWS stations. The time series data are available at https://figshare.com/s/35c46386b13ad5e26fe0.

References

Allen, R. M., Gasparini, P., Kamigaichi, O., & Böse, M. (2009). The status of earthquake early warning around the world: An introductory overview. *Seismological Research Letters*, *80*(5), 682–693. https://doi.org/10.1785/gssrl. 80.5.682

Böse, M., Heaton, T., & Hauksson, E. (2012). Rapid estimation of earthquake source and ground-motion parameters for earthquake early warning using data from a single three-component broadband or strong-motion sensor. *Bulletin of the Seismological Society of America*, *102*(2), 738–750. https://doi.org/10.1785/0120110152

Carranza, M., Buforn, E., Colombelli, S., & Zollo, A. (2013). Earthquake early warning for southern Iberia: A *P* wave threshold-based approach. *Geophysical Research Letters*, *40*, 4588–4593. https://doi.org/10.1002/grl.50903

Caruso, A., Colombelli, S., Elia, L., Picozzi, M., & Zollo, A. (2017). An on-site alert level early warning system for Italy. *Journal of Geophysical Research: Solid Earth*, *122*, 2106–2118. https://doi.org/10.1002/2016JB013403

Emolo, A., Picozzi, M., Festa, G., Martino, C., Colombelli, S., Caruso, A., et al. (2016). Earthquake early warning feasibility in the Campania region (southern Italy) and demonstration system for public school buildings. *Bulletin of Earthquake Engineering*, *14*(9), 2513–2529. https://doi.org/10.1007/s10518-016-9865-z

Hsu, T. Y., Huang, S. K., Chang, Y. W., Kuo, C. H., Lin, C. M., Chang, T. M., et al. (2013). Rapid on-site peak ground acceleration estimation based on support vector regression and *P*-wave features in Taiwan. *Soil Dynamics and Earthquake Engineering*, *49*, 210–217. https://doi.org/10.1016/j.soildyn. 2013.03.001

Hsu, T. Y., Wang, H. H., Lin, P. Y., Lin, C. M., Kuo, C. H., & Wen, K. L. (2016). Performance of the NCREE's on-site warning system during the 5 February 2016 M_w 6.53 Meinong earthquake. *Geophysical Research Letters*, *43*, 8954–8959. https://doi.org/10.1002/2016GL069372

Kanamori, H. (2005). Real-time seismology and earthquake damage mitigation. *Annual Review of Earth and Planetary Sciences*, *33*(1), 195–214. https://doi.org/10.1146/annurev.earth.33.092203.122626

Meier, M. A. (2017). How "good" are real-time ground motion predictions from earthquake early warning systems? *Journal of Geophysical Research: Solid Earth*, *122*, 5561–5577. https://doi.org/10.1002/2017JB014025

Nakamura, Y. (1998). A new concept for the earthquake vulnerability estimation and its application to the early warning system, *Proc Early Warning Conf Potsdam*, Germany.

Odaka, T., Ashiya, K., Tsukada, S., Sato, S., Ohtake, K., & Nozaka, D. (2003). A new method of quickly estimating epicentral distance and magnitude from a single seismic record. *Bulletin of the Seismological Society of America*, *93*(1), 526–532. https://doi.org/10.1785/0120020008

Peng, C., Yang, J., Chen, Y., Zhu, X., Xu, Z., Zheng, Y., & Jiang, X. (2015). Application of a threshold-based earthquake early warning method to the M_w 6.6 Lushan earthquake, Sichuan, China. *Seismological Research Letters*, *86*(3), 841–847. https://doi.org/10.1785/0220140053

Wu, Y. M., Chen, D. Y., Lin, T. L., Hsieh, C. Y., Chin, T. L., Chang, W. Y., & Ker, S. H. (2013). A high-density seismic network for earthquake early warning in Taiwan based on low cost sensors. *Seismological Research Letters*, *84*(6), 1048–1054. https://doi.org/10.1785/0220130085

Wu, Y. M., Teng, T. L., Shin, T. C., & Hsiao, N. C. (2003). Relationship between peak ground acceleration, peak ground velocity, and intensity in Taiwan. *Bulletin of the Seismological Society of America*, *91*(5), 1218–1228.

Zollo, A., Amoroso, O., Lancieri, M., Wu, Y. M., & Kanamori, H. (2010). A threshold-based earthquake early warning using dense accelerometer networks. *Geophysical Journal International*, *183*(2), 963–974. https://doi.org/10.1111/j.1365-246X.2010.04765.x

Geophysical Research Letters

Supporting Information for

Comparing the Performance of the NEEWS Earthquake Early Warning System Against the CWB System During the February 6 2018 Mw 6.4 Hualien Earthquake

T. Y. Hsu[1,2], P. Y. Lin[2], H. H. Wang[2], H. W. Chiang[2], Y. W. Chang[2], C. H. Kuo[2], C. M. Lin[2], and K. L. Wen[2,3]

[1] Department of Civil and Construction Engineering, National Taiwan University of Science and Technology, Taiwan.

[2] National Center for Research on Earthquake Engineering, Taiwan.

[3] Department of Earth Sciences, National Central University, Taiwan.

Contents of this file

Introduction

This supporting information provides measured acceleration time history of the component with maximum PGA at the 28 NEEWS stations during the 2018 Hualian earthquake in Taiwan which caused 17 deaths (S1 to S7). In addition, the distribution of PGA difference is also shown to display the directivity associated with the earthquake source rupture direction (S8).

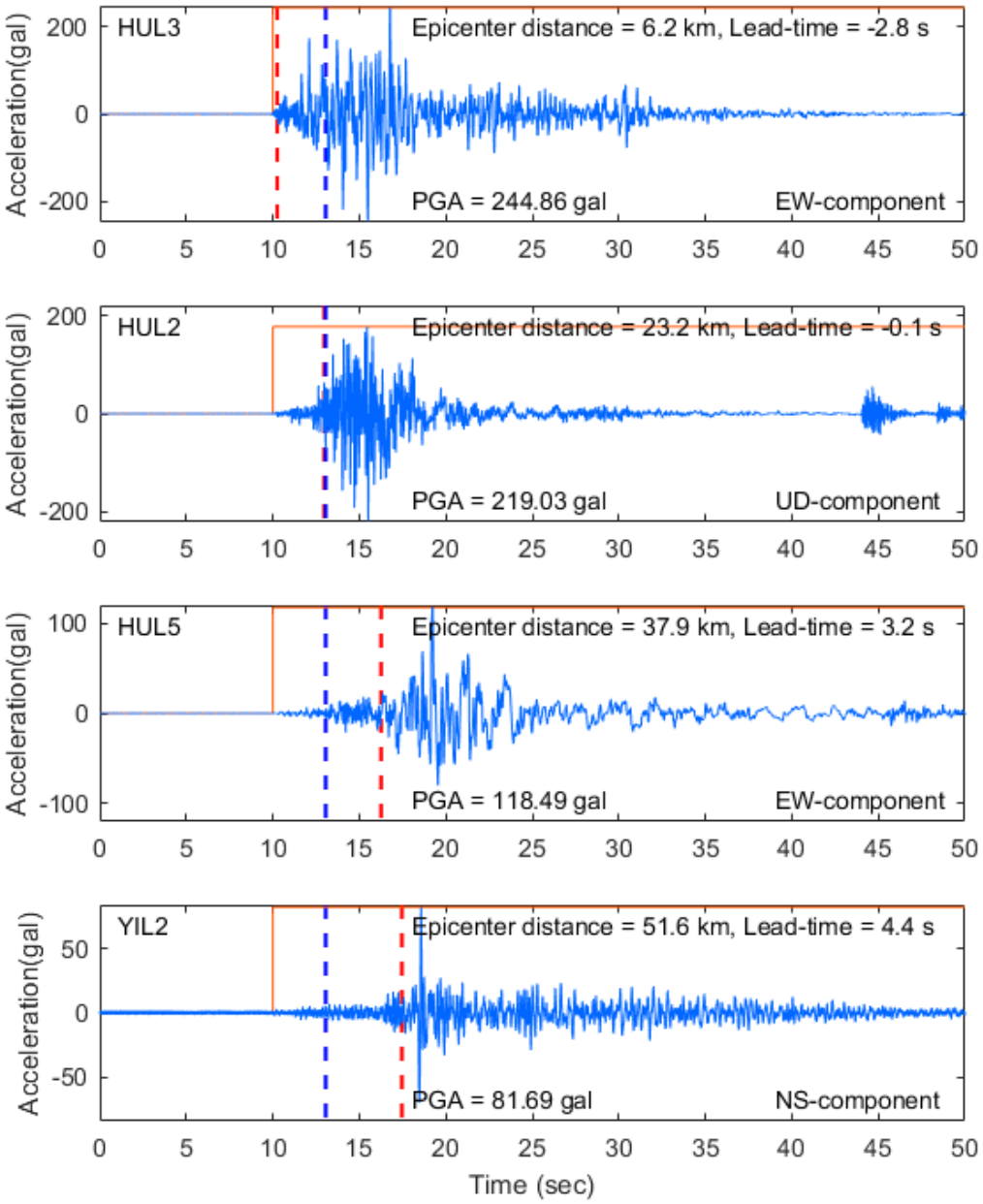

Figure S1. Measured acceleration time history of the component with maximum PGA at the 28 NEEWS stations, as sequenced by epicenter distance. Time when an alert was issued and arrival of the S-wave are denoted in dotted blue and dotted red lines, respectively. The orange envelope represents the phase during which the system was triggered. No alert was issued at Stations TAN3 and PIT1 because the phase duration was less than 3 s once the system was triggered; hence, the lead time of these two stations was zero. Part 1: the first 1~4 stations.

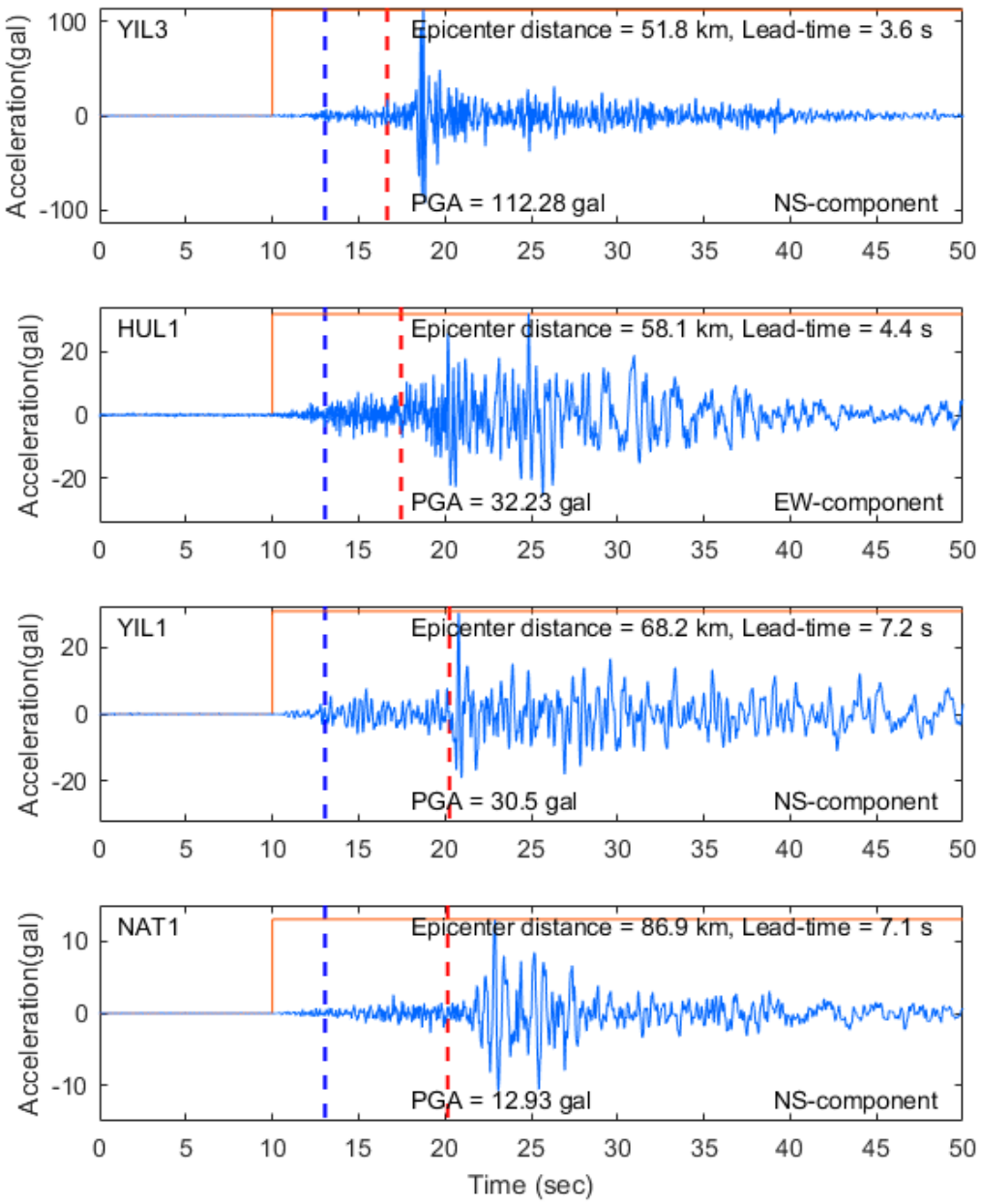

Figure S2. Measured acceleration time history of the component with maximum PGA at the 28 NEEWS stations, as sequenced by epicenter distance. Time when an alert was issued and arrival of the S-wave are denoted in dotted blue and dotted red lines, respectively. The orange envelope represents the phase during which the system was triggered. No alert was issued at Stations TAN3 and PIT1 because the phase duration was less than 3 s once the system was triggered; hence, the lead time of these two stations was zero. Part 1: the first 5~8 stations.

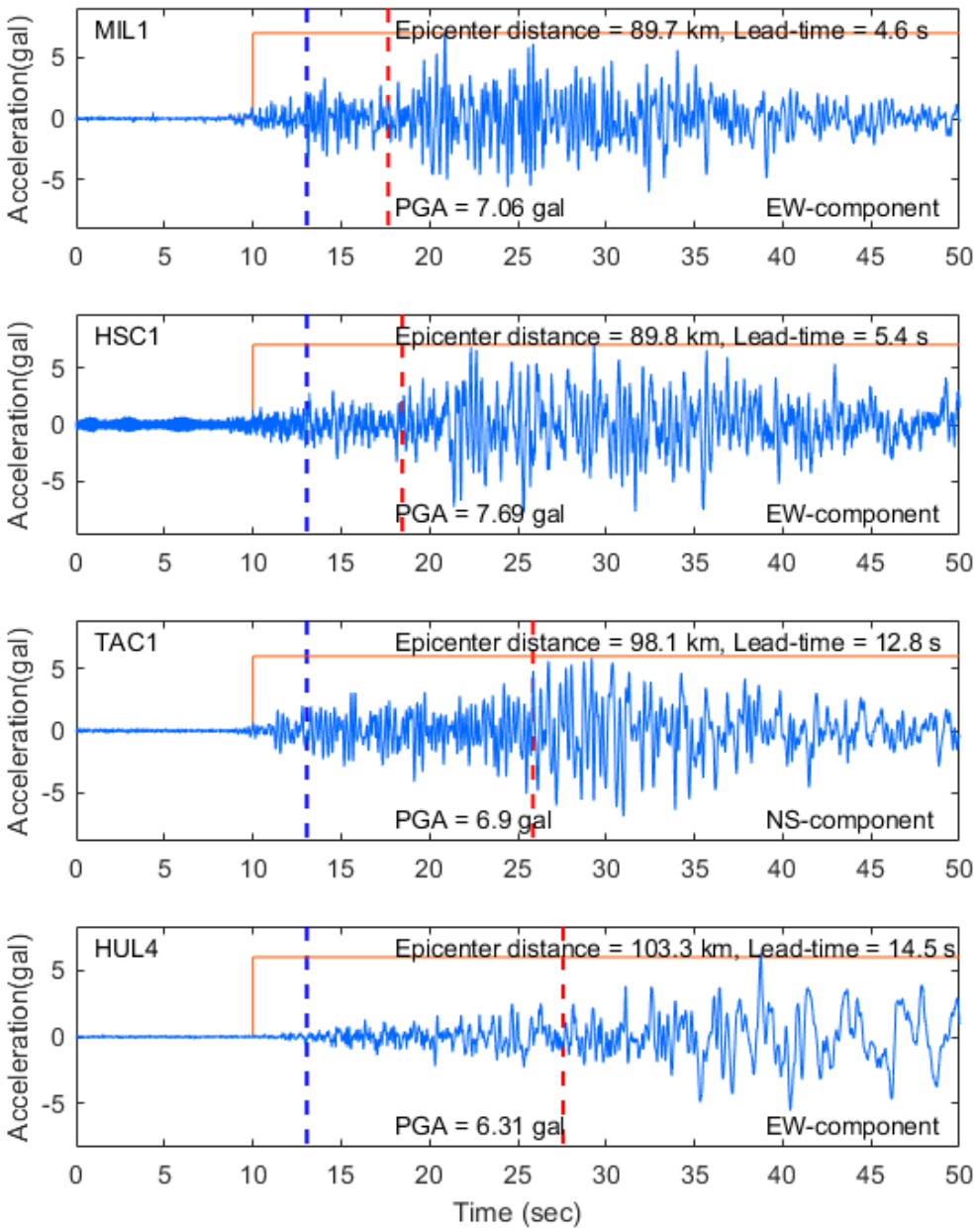

Figure S3. Measured acceleration time history of the component with maximum PGA at the 28 NEEWS stations, as sequenced by epicenter distance. Time when an alert was issued and arrival of the S-wave are denoted in dotted blue and dotted red lines, respectively. The orange envelope represents the phase during which the system was triggered. No alert was issued at Stations TAN3 and PIT1 because the phase duration was less than 3 s once the system was triggered; hence, the lead time of these two stations was zero. Part 1: the first 9~12 stations.

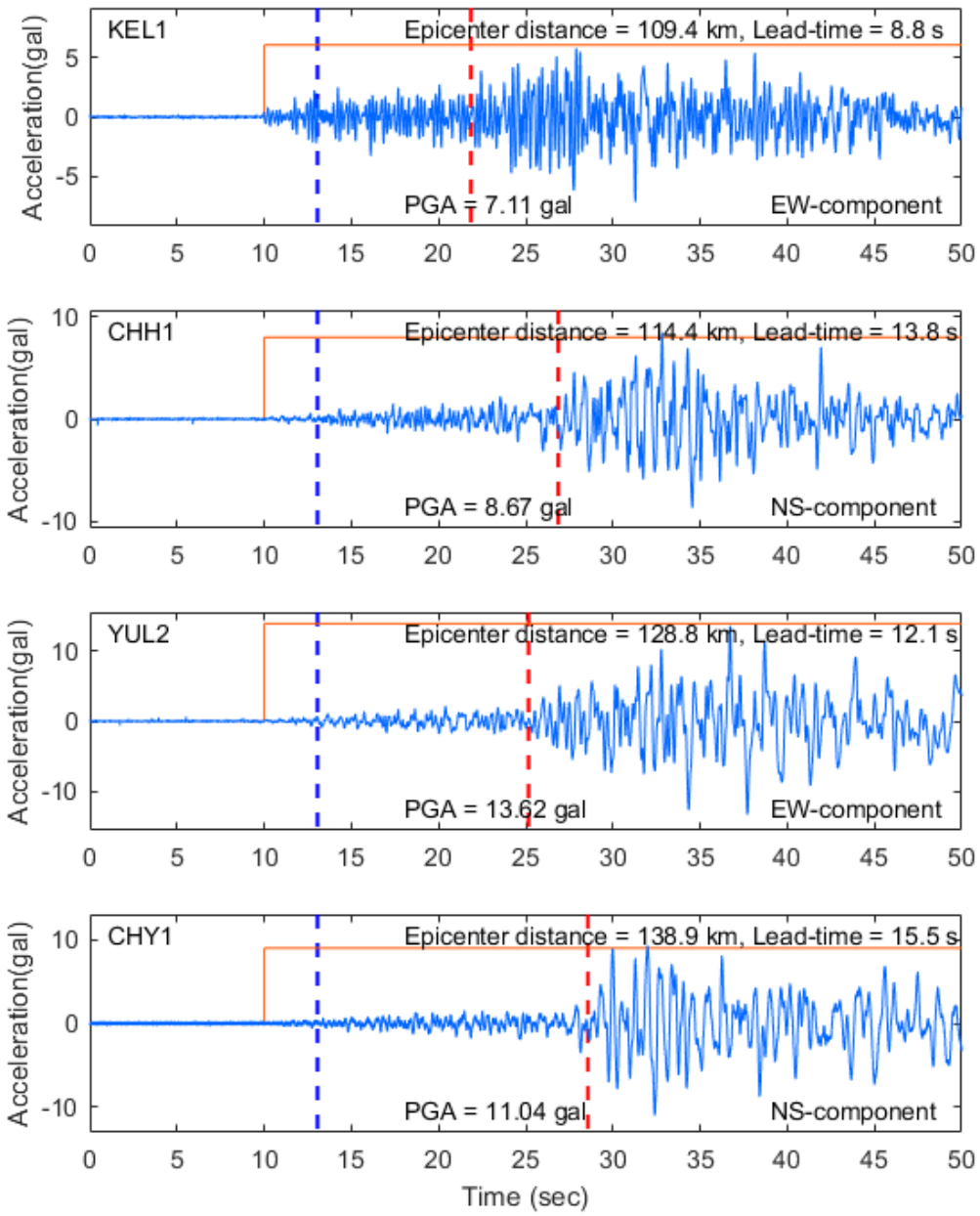

Figure S4. Measured acceleration time history of the component with maximum PGA at the 28 NEEWS stations, as sequenced by epicenter distance. Time when an alert was issued and arrival of the S-wave are denoted in dotted blue and dotted red lines, respectively. The orange envelope represents the phase during which the system was triggered. No alert was issued at Stations TAN3 and PIT1 because the phase duration was less than 3 s once the system was triggered; hence, the lead time of these two stations was zero. Part 1: the first 13~16 stations.

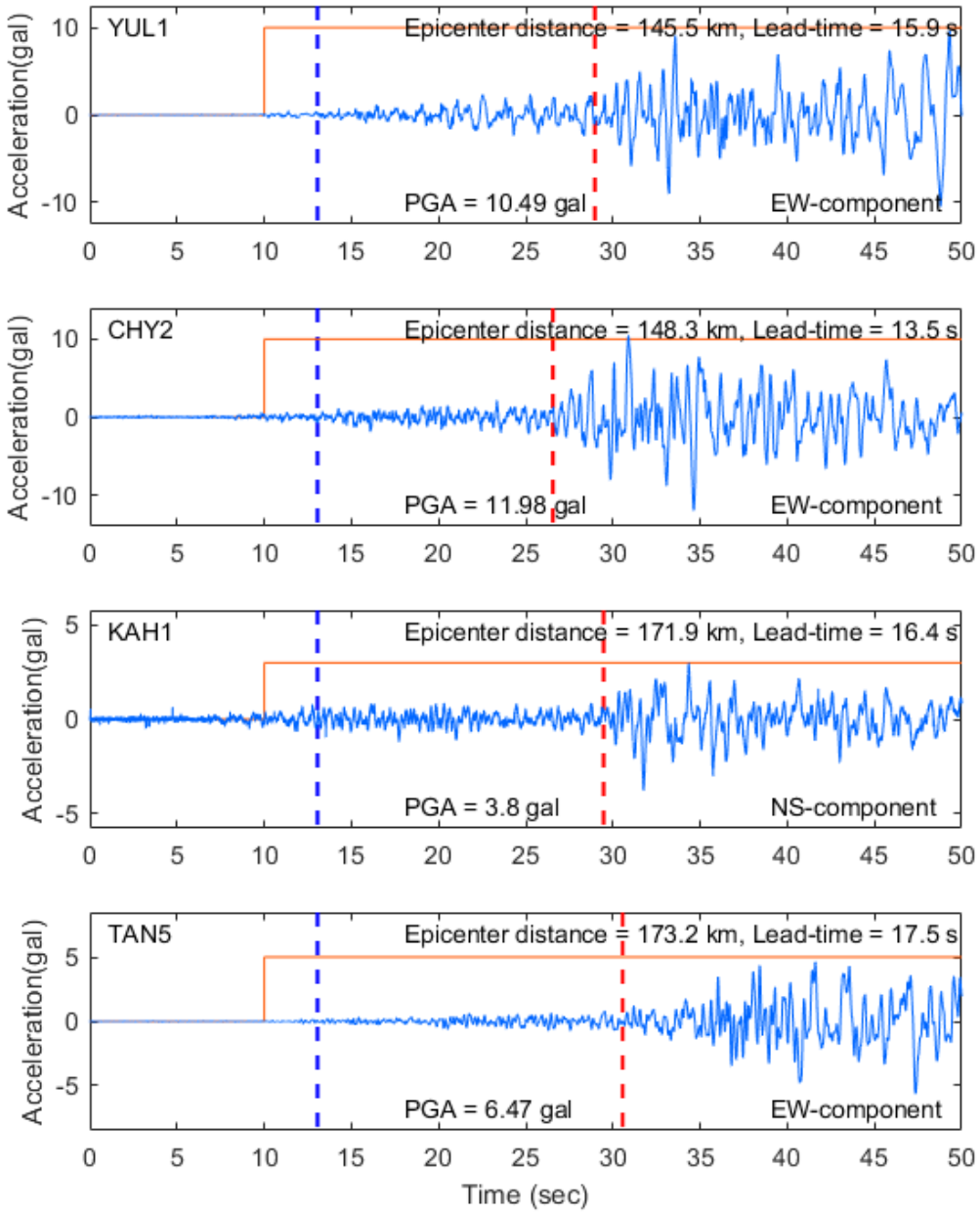

Figure S5. Measured acceleration time history of the component with maximum PGA at the 28 NEEWS stations, as sequenced by epicenter distance. Time when an alert was issued and arrival of the S-wave are denoted in dotted blue and dotted red lines, respectively. The orange envelope represents the phase during which the system was triggered. No alert was issued at Stations TAN3 and PIT1 because the phase duration was less than 3 s once the system was triggered; hence, the lead time of these two stations was zero. Part 1: the first 17~20 stations.

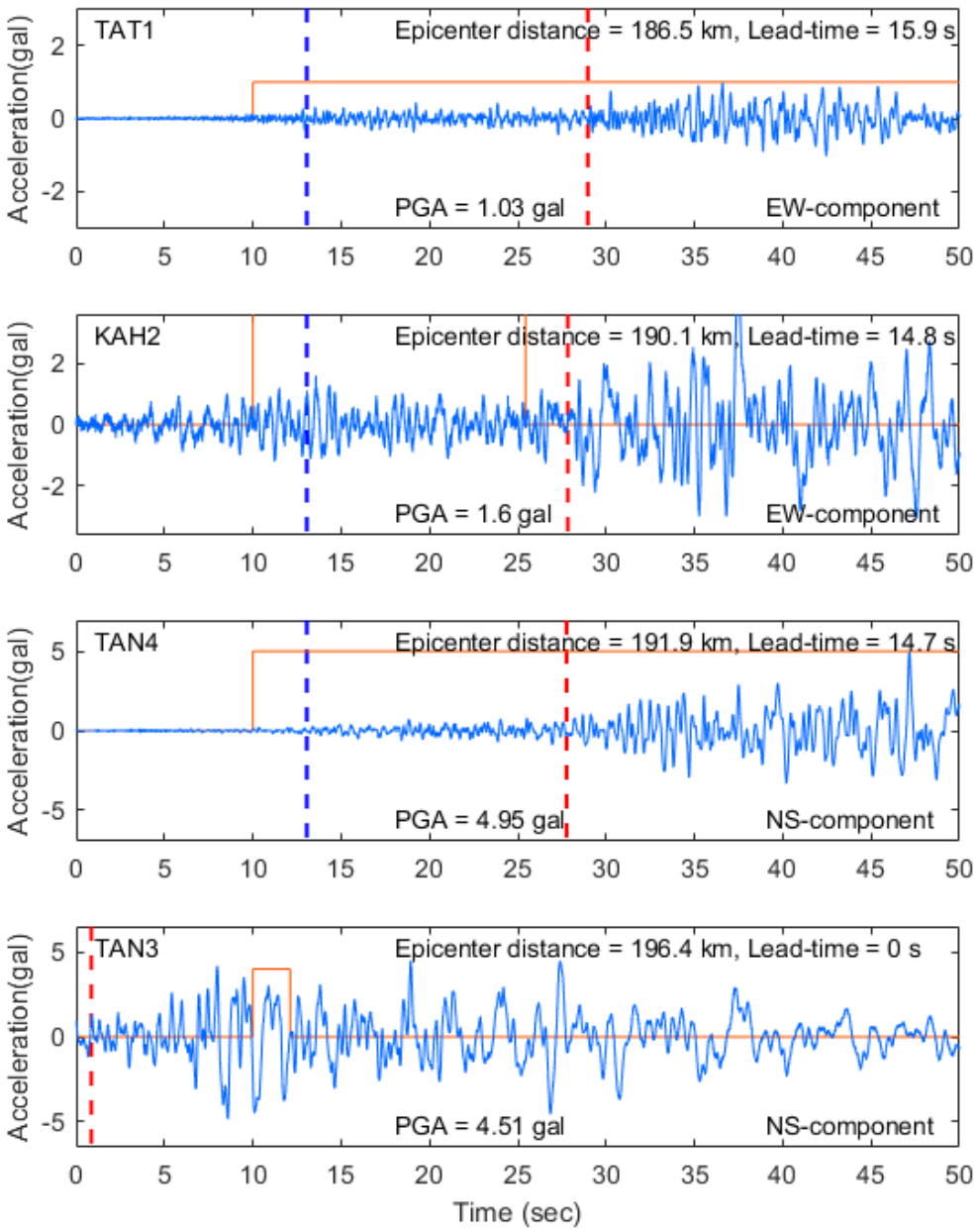

Figure S6. Measured acceleration time history of the component with maximum PGA at the 28 NEEWS stations, as sequenced by epicenter distance. Time when an alert was issued and arrival of the S-wave are denoted in dotted blue and dotted red lines, respectively. The orange envelope represents the phase during which the system was triggered. No alert was issued at Stations TAN3 and PIT1 because the phase duration was less than 3 s once the system was triggered; hence, the lead time of these two stations was zero. Part 1: the first 21~24 stations.

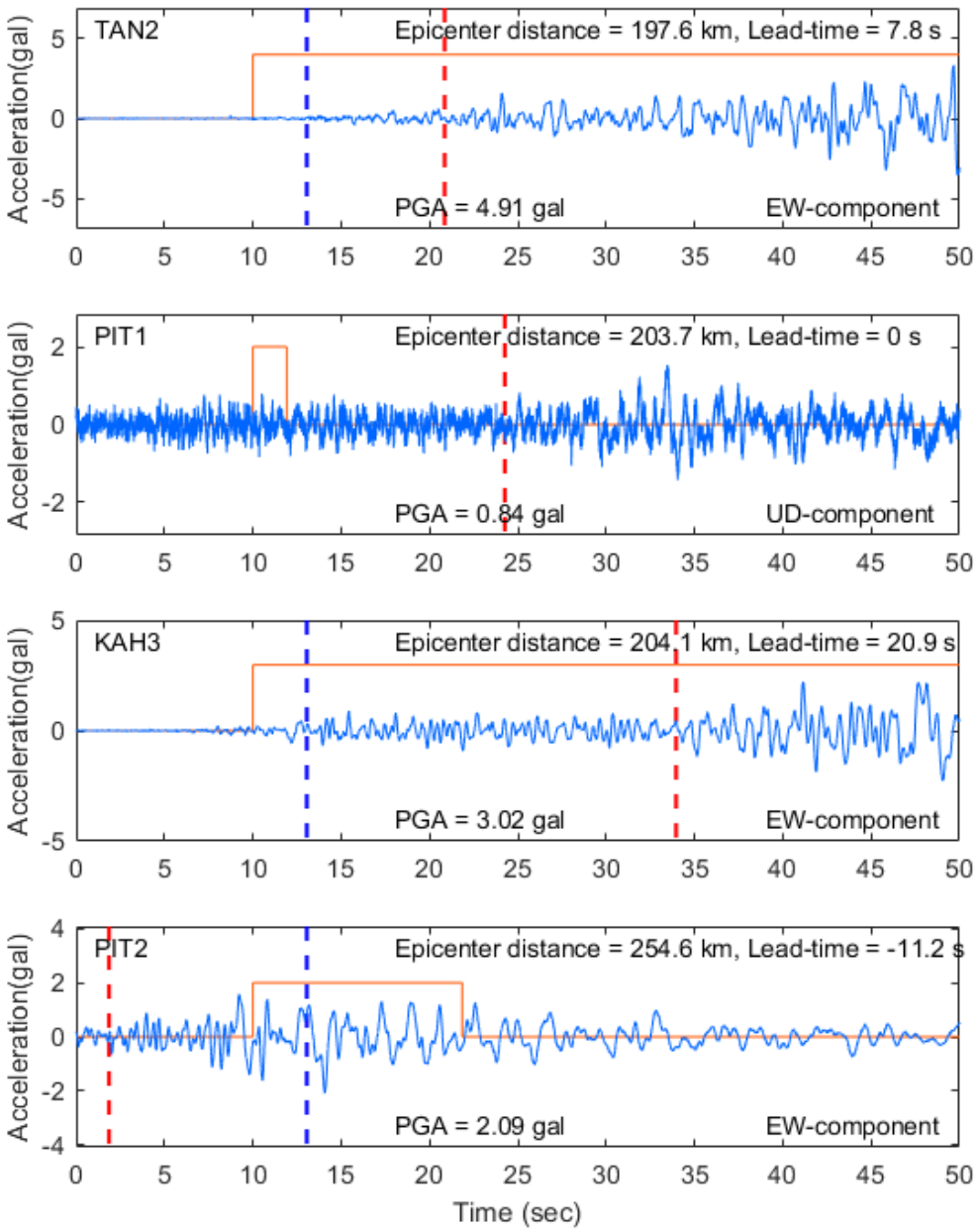

Figure S7. Measured acceleration time history of the component with maximum PGA at the 28 NEEWS stations, as sequenced by epicenter distance. Time when an alert was issued and arrival of the S-wave are denoted in dotted blue and dotted red lines, respectively. The orange envelope represents the phase during which the system was triggered. No alert was issued at Stations TAN3 and PIT1 because the phase duration was less than 3 s once the system was triggered; hence, the lead time of these two stations was zero. Part 1: the first 25~28 stations.

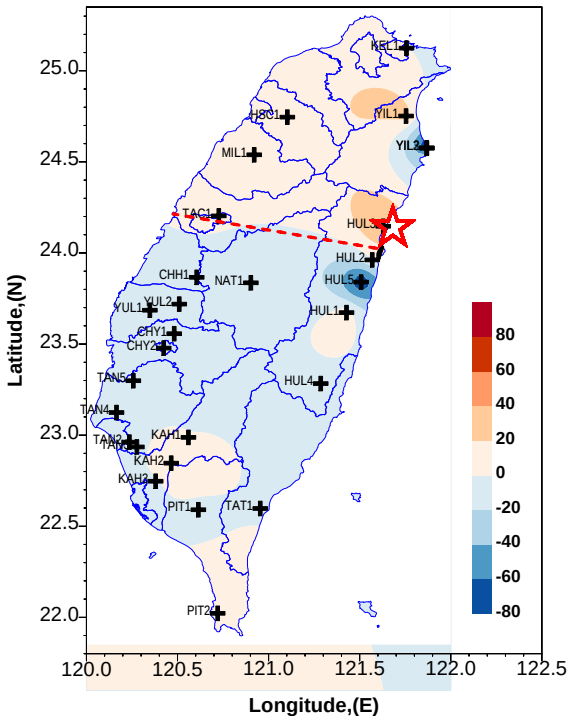

Figure S8. Distribution of PGA difference. The PGA difference is defined as the predicted PGA of the NEEWS minus the measured PGA in gals. Most PGA differences in the southern regions (separated by the red line) were negative. By contrast, all PGA differences in the northern regions were positive, indicating that directivity effects dominate.